A Diagnostic Model for Estimating Large-Scale Flow Patterns in the Tropical Upper Troposphere from Satellite Cloud Brightness Data

C.-P. CHANG, F. T. JACOBS, AND B. B. EDWARDS

Department of Meteorology, Naval Postgraduate School, Monterey, Calif. 93940

(Manuscript received 6 November 1974; in revised form 27 February 1975)

ABSTRACT

A diagnostic model is proposed to use digitized satellite cloud brightness data to estimate objectively the large-scale flow patterns over data-void tropical regions. The model utilizes a linear barotropic vorticity equation with two primary assumptions: 1) that the area-averaged cloud brightness is positively correlated with large-scale divergence in the tropical upper troposphere; and 2) that the large-scale tropical flow is quasi-barotropic and quasi-non-divergent. It is designed to be used at any upper tropospheric level where divergence is important in determining the vorticity field. Three types of information are required: 1) boundary conditions determined from surrounding wind reports, 2) a mean zonal flow determined from climatology, and 3) an equivalent divergence forcing function constructed empirically from the brightness data.

The model is tested daily over a western North Pacific region for July-August 1971. Results for an 8-day representative period are presented and discussed. In general for 25% of the days tested, the model produces a flow field which accurately resembles the major features of the streamfunction field analyzed by the National Meteorological Center. In another 30% of the days it provides some valuable information about the flow patterns which would be difficult to obtain from boundary information alone. Experiments are also performed for two days in which the brightness data are enhanced by time-interpolated satellite infrared data. The resultant flow fields bear better resemblance to the NMC analysis. It is thus suggested that improved results may be expected when infrared and other types of advanced satellite data are available.

1. Introduction

Satellite photographs of tropical regions have revealed that much of the tropical cloudiness is in the form of large, connected masses of very bright clouds. These masses are composed of many individual cumulus clouds, whose extensive cirrus canopies with a horizontal scale of several hundred kilometers or larger account for most of their brightness. These large, bright cloud masses, or "cloud clusters" as they are now called, have received considerable attention in recent years. Chang (1970) and Wallace (1970, 1971), using time-longitude series of satellite photographs, found that many cloud clusters over the tropical Pacific are well organized and have characteristics resembling those of synoptic-scale westward propagating wave disturbances. Further evidence by Reed and Recker (1971) showed that these propagating cloud clusters in the western North Pacific are linked to synoptic-scale waves in the windfields. Williams and Gray (1973) and Yanai *et al.* (1973) have also deduced the mean properties of these western North Pacific cloud clusters and found that the vertical distributions of several physical variables of the active clusters are generally similar to those found by Reed and Recker (1971) and Nitta (1972) for the wave troughs.

Due to the poor radiosonde coverage over the vast tropical oceans, it is natural to try to use the available satellite data as an aid for tropical analysis. Digitized cloud brightness data have been available since 1967. They were first acquired by the Advanced Vidicon Camera System of the operational satellite system between 1967 and late summer 1972, and then by the two-channel Scanning Radiometer since November 1972. Because of the relationship between the bright cloud clusters and synoptic-scale tropical motions, these data become a potential source for such a purpose. In fact, evidence of relations between the satellite brightness data and other meteorological parameters has been found by several investigators. The correlation between brightness and precipitation has led to many attempts to estimate rainfall using satellite brightness (for example, see review by Martin and Scherer, 1973). Wallace (1971) also found indication of good correspondence between area-averaged cloud brightness and synoptic-scale vertical motion associated with the 4- to 5-day tropical disturbances in the Kwajalein-Eniwetok-Ponape triangle of the Marshall Islands and the Guam-Truk-Yap triangle further west. He postulated that it may be possible to obtain an estimate of the vertical motion field over the tropics from the cloud brightness data alone. If this turns out to be the case, the satellite cloud brightness data will certainly be one of the best available indicators of disturbed weather in the tropics.

There are physical reasons to think that brightness data is closely related to the large-scale vertical motion

field. The bright cirrus canopies associated with the cloud clusters "are produced by outflow from and remnants of cumulonimbi. In general, developing and conservative clusters maintain their cumulonimbi from a steady low-level mass convergence; clusters gradually die when their low-level mass convergence is eliminated" (Williams and Gray, 1973). Because of the readily available low-level moisture, the large-scale upward motion provides a favorable environment for the development and existence of the clusters. Furthermore, since the magnitude of the latent heating is nearly one order greater than the temperature fluctuations at most levels for large-scale, convectively-active tropical motions, thermal energy balance requires that the large-scale vertical motion must be approximately proportional to heating (Wallace, 1971; Holton, 1972). Thus one could expect a positive correlation between cloud brightness and large-scale vertical motion by reason of heating alone.

The correspondence between brightness and vertical motion may also be extended to large-scale horizontal divergence at levels where divergence is large, since many observational studies (Wallace, 1971; Reed and Recker, 1971; Nitta, 1972; Williams and Gray, 1973; Yanai *et al.*, 1973; Reed and Johnson, 1974) have produced very similar profiles of the vertical motion (or divergence) over tropical areas where convection is active. The same conclusion can also be inferred from the various vertical heating profiles shown by Hayashi (1974) from analyses of tropical output from the general circulation model of the NOAA Geophysical Fluid Dynamics Laboratory at Princeton. In addition, Williams and Gray (1973) have shown a clear in-phase relation between cloud clusters and upper-level divergence in their composite study.

So far, the use of satellite brightness data as an aid to tropical analysis has been limited to subjective methods only; i.e., an analyst relying on visual inspection of the satellite photographs to modify conventional weather maps. If the digitized brightness data can be used to estimate the large-scale vertical motion, as postulated by Wallace, and upper-level divergence, as reasoned above, then there may be ways to use this digitized data in an objective manner. The purpose of this study is to propose such a model, in which the digitized brightness will be used to objectively diagnose the large-scale flow pattern in the tropical upper troposphere, over regions where wind reports are sparse or void.[1]

2. The basic model

The diagnostic model of using digitized satellite cloud brightness to detect large-scale tropical flow is based on two primary suppositions:

1) Brightness is positively correlated with active convection, and therefore with large-scale condensation heating, vertical motion, and upper-level divergence.

2) Large-scale tropical flow is usually quasi-barotropic and quasi-non-divergent.

The model used is essentially a linearized barotropic vorticity equation which may be applied at any level where divergence is relatively important in determining the rotational part of the flow, such as the maximum-divergence level or the "outflow" level of the cloud clusters, usually near 200 mb in the tropics. It is similar to the simple diagnostic model by Holton and Colton (1972) for the 200 mb seasonal mean circulations during the northern summer, in which the mean motion field was successfully reproduced by the steady-state solution of a linearized barotropic vorticity equation with observed mean divergence and mean zonal wind. In our model the vorticity equation is applied to a data-void region on a daily basis, with horizontal divergence replaced by an "equivalent divergence" field derived from the brightness data, basic zonal wind given by climatology, and boundary conditions determined by the data-rich surrounding areas. Similar to Holton and Colton's time-mean model, a damping coefficient is introduced to parameterize the strong damping process in the tropical upper troposphere as reported by several vorticity budget studies (Reed and Recker, 1971; Williams and Gray, 1973; and others). We hope this model can reasonably describe the rotational part of the large-scale motion near the outflow level, and it may be useful for diagnostic purposes if we know what kind of solution can best approximate the actual motion field at the satellite observation time. If 12 h or 24 h history is available (presumably by use of this technique at an earlier time or by some other means), extrapolation in time may be used. However, the previous vorticity budget studies have consistently shown that the local change of vorticity near the maximum-divergence level is rather small when compared to other terms in the vorticity equation. Hence, a diagnosis of the flow at this level over the data-void region may be acquired by way of a steady-state solution, which may be obtained by applying the initial-value technique to the vorticity equation. We hope that this solution may, to some degree, resemble the actual flow pattern and can be useful for large-scale tropical analysis as a first estimate of the upper-level flow over a data-void region.

The design of the model begins from the linearized barotropic vorticity equation,

$$\frac{\partial}{\partial t}\nabla^2\psi+\bar{u}\frac{\partial}{\partial x}\nabla^2\psi-\frac{\partial\psi}{\partial x}\frac{\partial^2\bar{u}}{\partial y^2}+\beta\frac{\partial\psi}{\partial x}=-\left(f-\frac{\partial\bar{u}}{\partial y}\right)B-\bar{B}\nabla^2\psi-D\nabla^2\psi, \quad (1)$$

[1] After completion of this work, Prof. J. M. Wallace informed us that Ambroziak (1973) has tested similar concepts in an unpublished work. However, his model used a quasi-prediction technique which implies somewhat different physical assumptions for the relation between heating and large-scale flow. His results are thus of a different type and they are generally less satisfactory as compared to those of the present model.

where the symbols have the following meaning:

ψ perturbation streamfunction
$\zeta=\nabla^2\psi$ perturbation relative vorticity
$\bar{u}$ mean zonal wind
f Coriolis parameter
$\beta=\partial f/\partial y$
B perturbation divergence
$\bar{B}$ zonal mean divergence
D a damping coefficient
x,y,t zonal, meridional directions and time, respectively.

In Eq. (1) the advections due to mean meridional velocity, mean vertical velocity, and the divergent part of the perturbation meridional velocity are all neglected from scale considerations. The term $-D\nabla^2\psi$ is included to represent the strong damping process in the upper troposphere as found by the budget studies. It is also consistent with the in-phase relationship between divergence and vorticity near the outflow level observed by Wallace (1971), because such a relationship requires the magnitude of the damping to be comparable to the divergence forcing (Holton and Colton, 1972). This damping process has not been fully understood. It may be due to strong cumulus transport of low-level vorticity as suggested by Reed and Recker (1971) and Holton and Colton (1972), or it may also be due to some other nonlinear processes. In their study Holton and Colton found that a very strong viscous damping coefficient, $D=1.5\times10^{-5}\,\mathrm{s}^{-1}$, is necessary in order to compute a realistic seasonal mean streamfunction field from the observed mean divergence. Other budget studies (for example, see Williams and Gray) also indicate that D in cloud-cluster areas is considerably larger than what may be expected for the usual large-scale damping time alone.

The corresponding finite-difference equation of (1), expressed by central differencing in both time and space (except that an implicit scheme is used for the damping term due to stability requirement), is

$$(\nabla^2\psi_{i,j})^{\tau+1}=\frac{(\nabla^2\psi_{i,j})^{\tau-1}[1-\Delta t(\bar{B}+D)]}{[1+\Delta t(\bar{B}+D)]}$$
$$+\frac{2\Delta t}{[1+\Delta t(\bar{B}+D)]}\cdot\left\{\left(-\frac{\bar{u}m}{2d}\right)(\nabla^2\psi_{i+1,j}-\nabla^2\psi_{i-1,j})\right.$$
$$+\left(\frac{m}{2d}\right)(\psi_{i+1,j}-\psi_{i-1,j})(\bar{u}_{j+1}-2\bar{u}_j+\bar{u}_{j-1})$$
$$+\left(-\frac{\beta d}{2m}\right)(\psi_{i+1,j}-\psi_{i-1,j})-\left(\frac{Bd^2}{m^2}\right)$$
$$\left.\cdot\left[f-\left(\left(\frac{m}{2d}\right)(\bar{u}_{j+1}-\bar{u}_{j-1})\right)\right]\right\}^{\tau}, \quad (2)$$

where

τ index for time step
i,j grid point indices in x and y, respectively
m map factor (equal to unity at 22.5°N throughout this study)
d grid interval, same for both x and y (equal to 2.5° at 22.5°N throughout the study).

Equation (2) may now be integrated in time over a rectangular region provided that $\bar{u}$, divergence ($\bar{B}$ and B), initial conditions, and proper boundary conditions are given. Two neighboring boundary conditions of ψ are required at both eastern and western boundaries because of the zonal advection term.

Since we will be looking for steady-state solution under forcing, the initial conditions will not be crucial and are always set to zero for the interior in this study. The specification of $\bar{u}$ poses a problem because it is assumed that we are dealing with a data-void region. However, it may be adequate to use values known from monthly or seasonal mean climatology. The divergence field, which is required as a forcing function for (2), will be given by an equivalent divergence field empirically constructed from digitized satellite brightness data. In the experiments of this model discussed in Section 4, three forcing fields for each day will be tested and results compared with the available NMC flow field: a divergence field kinematically computed from NMC-analyzed winds, an equivalent divergence field from brightness data, and a case of "zero forcing" where $\bar{B}=B=0$.

The specification of boundary conditions for ψ will depend upon the data available outside of the data-void region. We assume that, in most cases, the data-void region may be selected as a rectangular area or "box" surrounded on all four sides by boxes of arbitrary size within which wind information are adequate (see Fig. 1). These data-rich regions may be areas of island groups or edges of continents. If streamfunctions for each of these data-rich regions can be computed from the wind information, the boundary conditions of the

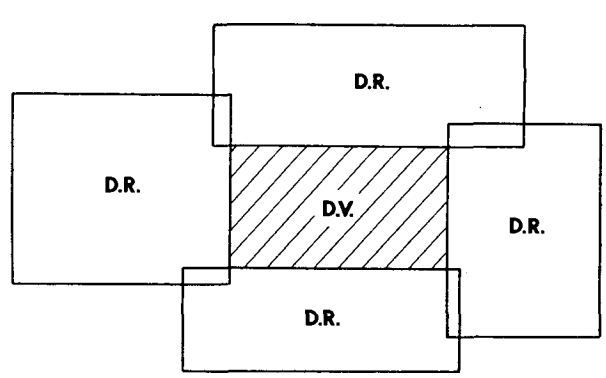

FIG. 1. Schematic diagram for computing boundary conditions of the data-void (DV) region from wind information of the surrounding data-rich (DR) regions.

data-void region can be determined because each of the four adjacent data-rich boxes shares one common border with the data-void box. There are many methods of computing the streamfunction from winds for a limited region. Among them the various versions of Sangster's (1960) method, as discussed by Hawkins and Rosenthal (1965), are all quite adequate for our purpose, especially Version III, which was found to give a streamfunction field closest to the NMC-analyzed field used in our test. We have also tried an iterative version of Sangster's method somewhat similar to that described by Shukla and Saha (1974), but the difference between the iterative and non-iterative version is usually small, and the additional computer time required for iteration is certainly not justified.

Although theoretically a method such as Sangster's must be used in the actual application of our technique, for simplicity the boundary conditions used in the numerous experiments carried out in this study are extracted directly from the available NMC-analyzed streamfunction field.

3. Period and area of study and data sources

In this study we used daily satellite brightness data for July–August 1971 to construct the forcing function for Eq. (2). The results are compared to the tropical grid wind data (including streamfunctions) analyzed by the National Meteorological Center (NMC). The area selected for this study is the tropical western North Pacific, from the equator to 25°N and 125°E to 175°E. This region was selected because of its 11 rawinsonde stations, including the Caroline and Marshall Islands, which make the NMC-analyzed wind data relatively more reliable compared to other areas of the tropics. Figure 2 shows the region and the rawinsonde network.

The digitized cloud brightness and upper-level wind data tapes were provided by the National Center for Atmospheric Research (NCAR). The cloud brightness data, acquired by NCAR from the National Environmental Satellite Service (NESS), are digitized values ranging from zero to ten averaged for 5°×5° latitude-longitude squares. The daily observation time is approximately 3 p.m. local time (~0000 GMT in the Western Pacific). The upper-level component winds as well as streamfunction fields at the 200 mb level were acquired by NCAR from the NMC tropical grid analysis. Since the NMC model weighs heavily its previous 12 h forecast to objectively analyze, and occasionally override, the observed data, the NMC analysis is not necessarily the correct solution for a given data set. However, it is the only available analysis we can use. Thus the NMC 200 mb streamfunction fields will be considered as the "observed fields" in this study. The wind and streamfunction values are given at grid points approximately coinciding with those for the brightness data, and are the results of analyses based on all available rawinsondes, aircraft observations, and a few winds deduced

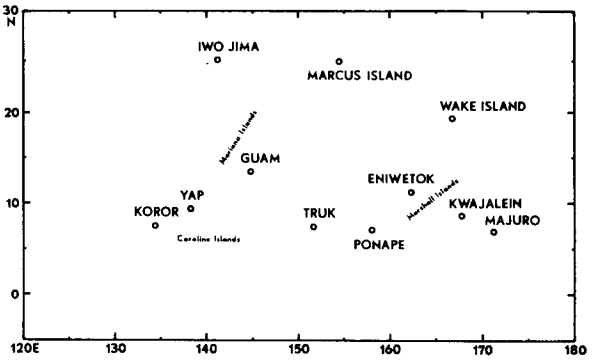

FIG. 2. Region of study and observational network.

from cloud drift as seen from satellite photographs. In all cases, the 0000 GMT wind data are considered as being closest to the time of satellite observations. All data are interpolated to give values at the 2.5°×2.5° latitude-longitude grid points used in this study to reduce truncation errors in the numerical integration. This process also has a smoothing effect on the forcing field. The mean zonal flow $\bar{u}$ required in (2) is computed by averaging the zonal component of the NMC winds over all longitudes in the region of study and over the three-month (June–August 1971) summer season.

Values for divergence are computed kinematically from the analyzed winds and found to be maximum at 200 mb. This is consistent with observational studies conducted by Reed and Recker (1971), Wallace (1971), Nitta (1972), Williams and Gray (1973), and Yanai *et al.* (1973), who all found that a non-divergent level is usually near 300 mb to 400 mb in the tropics and the 200 mb level is the outflow level with maximum divergence. Therefore, only the 200 mb level is tested in the experiments discussed in Section 4.

Before the observed satellite brightness data acquired from NCAR can be used as equivalent divergence forcing in (2), it must be related to the 200 mb divergence field. This is accomplished by a simple scheme. A proportionality factor K is computed by dividing the monthly standard deviation of divergence, σ_{div}, by the monthly standard deviation of brightness, σ_{CB}. The equivalent divergence at each grid point is then computed on a daily basis by the following equation,

$$(B+\bar{B})_E = K \cdot CB', \tag{3}$$

where

$(B+\bar{B})_E$ = equivalent divergence

CB' cloud brightness with seasonal mean brightness removed

$K = \dfrac{\sigma_{\text{div}}}{\sigma_{CB}}$ monthly proportionality constant.

When this equivalent divergence is used as forcing of (2), it will be referred to as "brightness forcing" in the discussion of the experiments in Section 4.

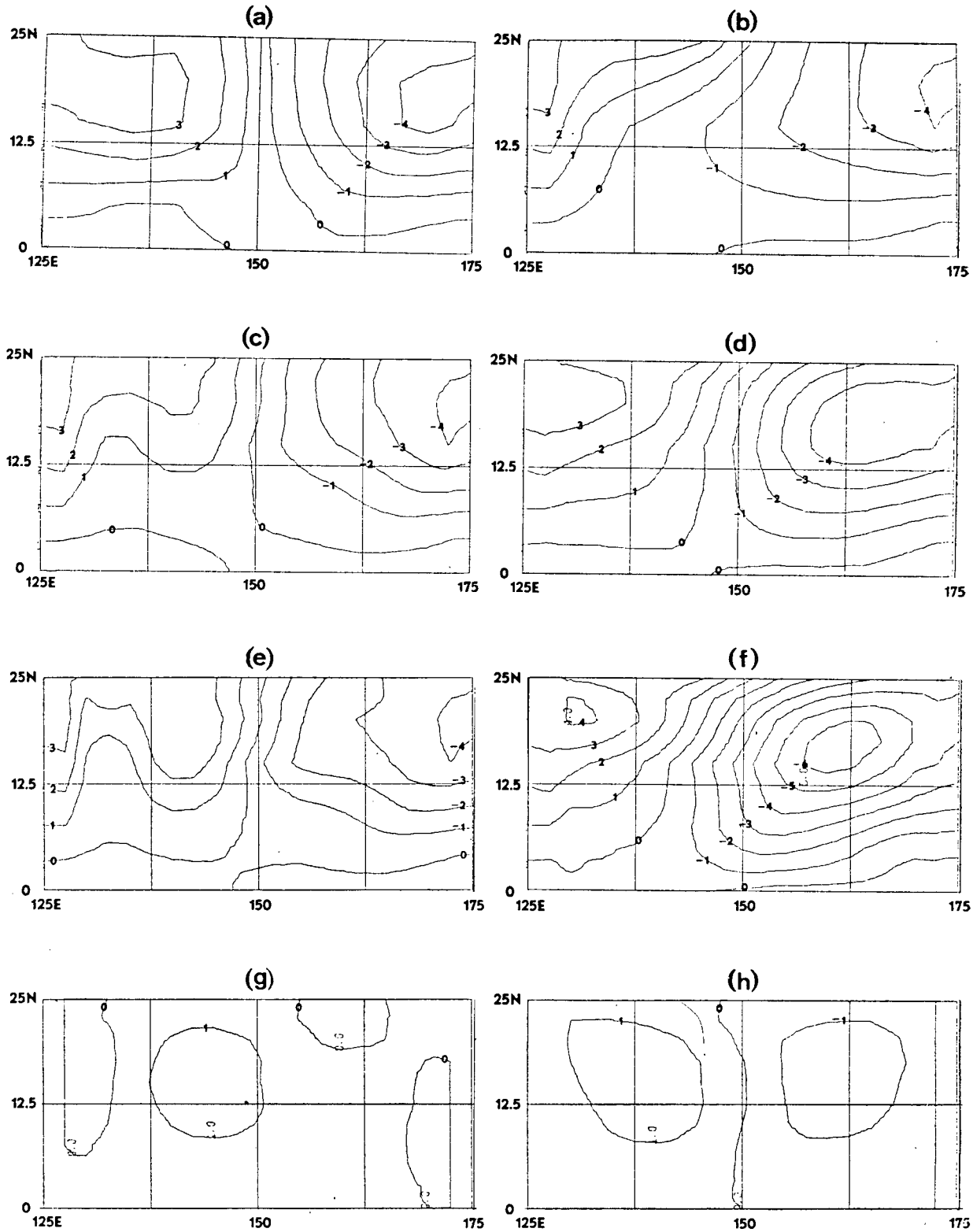

FIG. 3. Perturbation streamfunctions at 200 mb for 2 August 71 (contour interval is 5×10^{6} m^{2} s^{-1}). Fields shown are: (a) the NMC-analyzed field; and the 72 h solutions resulting from (b) zero forcing with $D=1.5\times10^{-5}$ s^{-1}, (c) divergence forcing with $D=1.5\times10^{-5}$ s^{-1}, (d) brightness forcing with $D=1.5\times10^{-5}$ s^{-1}, (e) divergence forcing with $D=5\times10^{-6}$ s^{-1}, (f) brightness forcing with $D=5\times10^{-6}$ s^{-1}, (g) divergence forcing with zero boundary conditions and $D=1.5\times10^{-5}$ s^{-1}, and (h) brightness forcing with zero boundary conditions and $D=1.5\times10^{-5}$ s^{-1}.

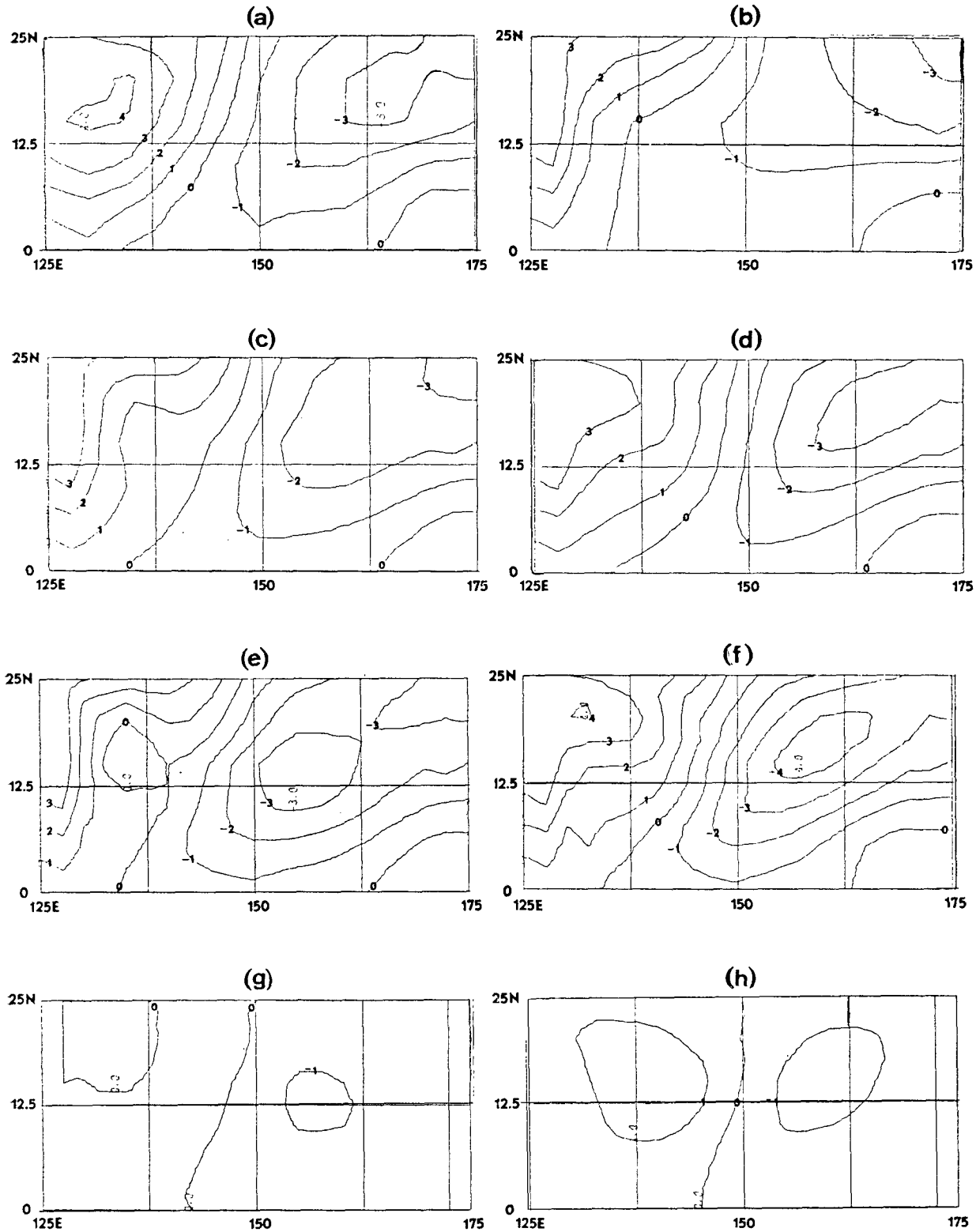

FIG. 4. Same as Fig. 3, except for 3 August 71.

The divergence and brightness used in this study have been analyzed in a correlation study by Varona (1974). Weak positive correlations between the two fields were found in space, time, and also for dominant time scales associated with synoptic disturbances in the period of study. However the correlation coefficients are much

lower than those inferred from Wallace's (1971) wave study. This may be due to the quality of the data used, especially the divergence which is kinematically computed from grid-point winds analyzed by NMC. We therefore expect that the results of experiments using divergence forcing and brightness forcing will generally be different. It turns out that in a number of cases the brightness forcing actually produces flow fields more closely resembling the observed field than those produced by our divergence data.

4. Results

a. Experiments with brightness forcing

In the daily diagnostic experiments three types of forcing functions are applied: the "divergence forcing" ($\bar{B}+B=$the kinematically computed divergence), the "brightness forcing" ($\bar{B}+B=$the equivalent divergence), and the "zero forcing" ($\bar{B}=B=0$). Quasi-steady-state solutions after 72 hours of integration are obtained for each day of July and August 1971, but only the results for an eight-day representative period are shown here (Figs. 3–10). These are the first eight days of August 1971 that have data available, namely 2, 3, 4, 5, 6, 7, 9, and 10 August. For each day of this period four computer-plotted diagrams of the perturbation streamfunction field are shown in the following order:

a) the NMC-analyzed field;
b) the solution for zero-forcing and $D=1.5\times10^{-5}$ s^{-1};
c) the solution for divergence forcing and $D=1.5\times10^{-5}$ s^{-1}; and
d) the solution for brightness forcing and $D=1.5\times10^{-5}$ s^{-1}.

For the first two days (2 and 3 August), the following four additional diagrams are also shown to compare with the first four diagrams:

e) the solution for divergence forcing and $D=5\times10^{-6}$ s^{-1};
f) the solution for brightness forcing and $D=5\times10^{-6}$ s^{-1};
g) the solution for divergence forcing, $D=1.5\times10^{-5}$ s^{-1}; and zero boundary conditions ($\psi=0$ at all boundaries); and
h) the solution for brightness forcing, $D=1.5\times10^{-5}$ s^{-1}, and zero boundary conditions.

The streamfunctions for 2 August are shown in Fig. 3. The solution obtained from brightness forcing (d) is quite similar to the NMC-analyzed field (a), with some differences in the strength of the major features but generally good agreement between gradients and flow patterns. On the other hand, the results of divergence forcing (c) show a good correspondence with the NMC field over the eastern half of the test region, but contains a fictitious trough in the northwestern "high" area. The zero-forcing solution (b) least resembles the NMC field, especially in the north-central sector where the flow displays excessive zonal orientation. As expected, the flow fields are too strong for both the divergence and brightness forcing when the damping coefficient is reduced to $D=5\times10^{-6}$ s^{-1} (e and f). The last two diagrams illustrate the results of the zero boundary condition cases. Here the brightness forcing (h) produces a pattern that better defines the distribution of positive and negative vorticity areas than does the divergence forcing (g), which is consistent with the results obtained when realistic boundary conditions are given.

Figure 4 shows the streamfunctions for 3 August. It can be seen that brightness forcing produces a flow field in excellent agreement with the NMC field for the entire region. The field produced by divergence suffers mainly from a fictitious trough which is present in the western "high" area. The zero-forcing solution again least resembles the NMC field. The results for smaller damping are again too strong. This is consistently true for all days tested. The value $D=1.5\times10^{-5}$ s^{-1} is thus considered an appropriate damping coefficient to be used in our model. The results for the zero boundary conditions, as expected, show that the brightness forcing better delineates the regions of negative and positive vorticity than does the divergence forcing.

The results for 4 August, as shown in Fig. 5, differ from those obtained on the two previous days. The field produced by brightness forcing does not agree as closely with the NMC field as it did on 2 and 3 August. Both the western and eastern "cells" are somewhat underdeveloped. However, the orientation of the eastern trough is better depicted by this field than by the field produced by the divergence or zero forcing, although the western anticyclonic circulation pattern produced by the divergence forcing more closely resembles that of the NMC field.

Results for 5 August are shown in Fig. 6. The major circulation features produced by the brightness forcing do not develop meridionally into the south central portion as those of the NMC field. This is particularly true of the southern extension of the -1 contour line of the eastern trough. Somewhat stronger development of this feature is produced by the divergence forcing. This feature is least developed in the solution obtained by zero-forcing; thus, on this day the brightness forcing result may still be considered as better than the zero-forcing case.

Figure 7 shows that for 6 August brightness forcing produces areas of anticyclonic vorticity over the western half and southeastern corner of the test region, both of which grossly resemble the patterns shown by the NMC field. However, the northeastern cyclonic circulation is overdeveloped by the brightness forcing. It can be seen that for this feature the zero-forcing solution has the closest agreement with the NMC field, but the overall resemblance is still best for the result of brightness forcing because of the two anticyclonic areas.

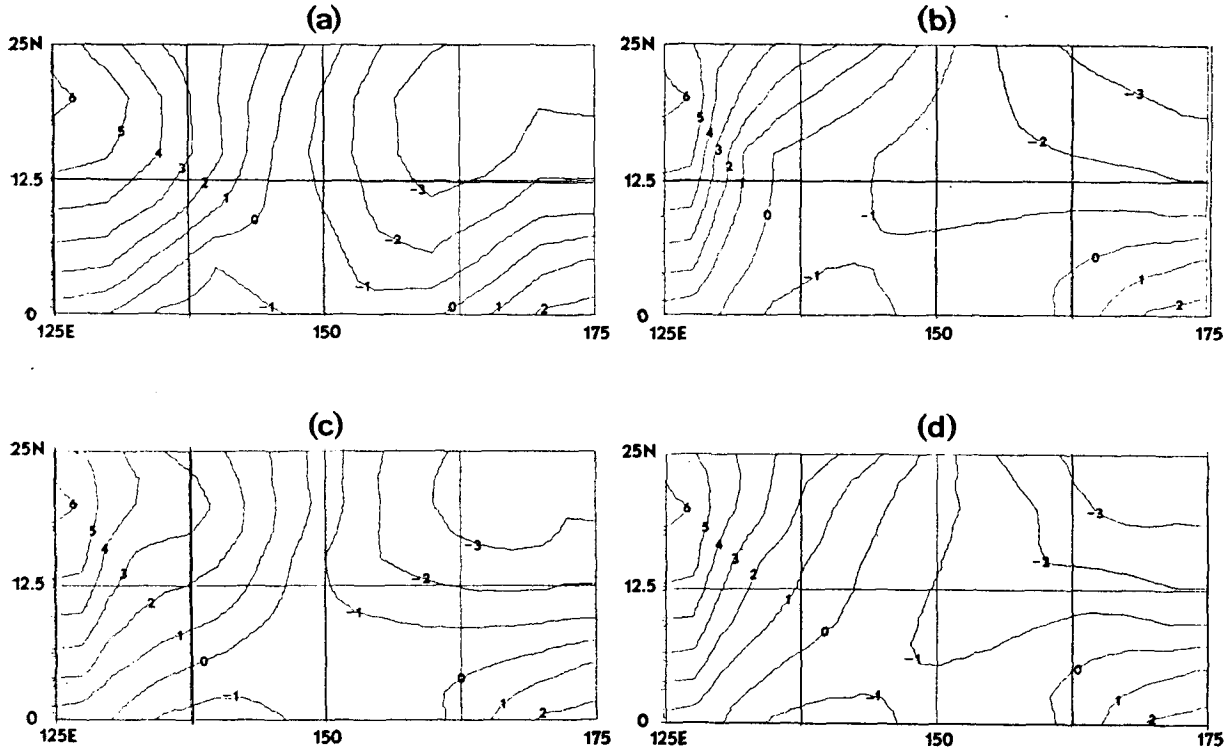

FIG. 5. Same as Fig. 3a–d, except for 4 August 71.

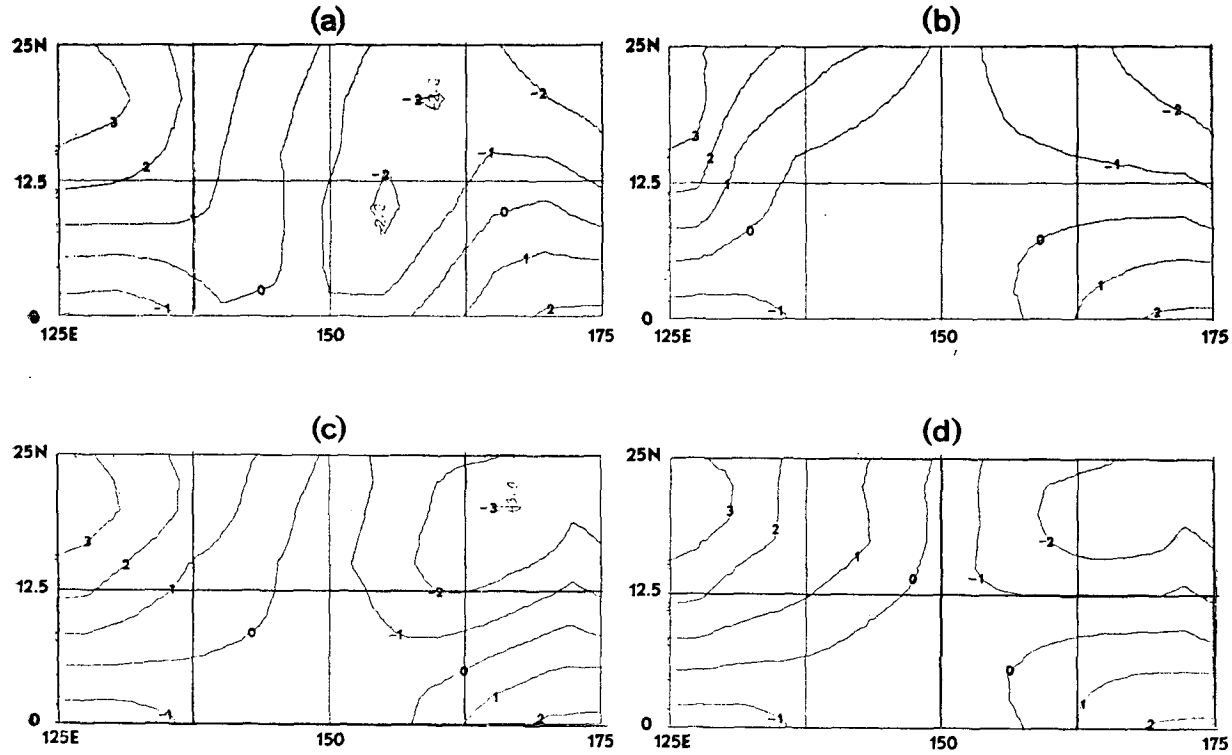

FIG. 6. Same as Fig. 3a–d, except for 5 August 71.

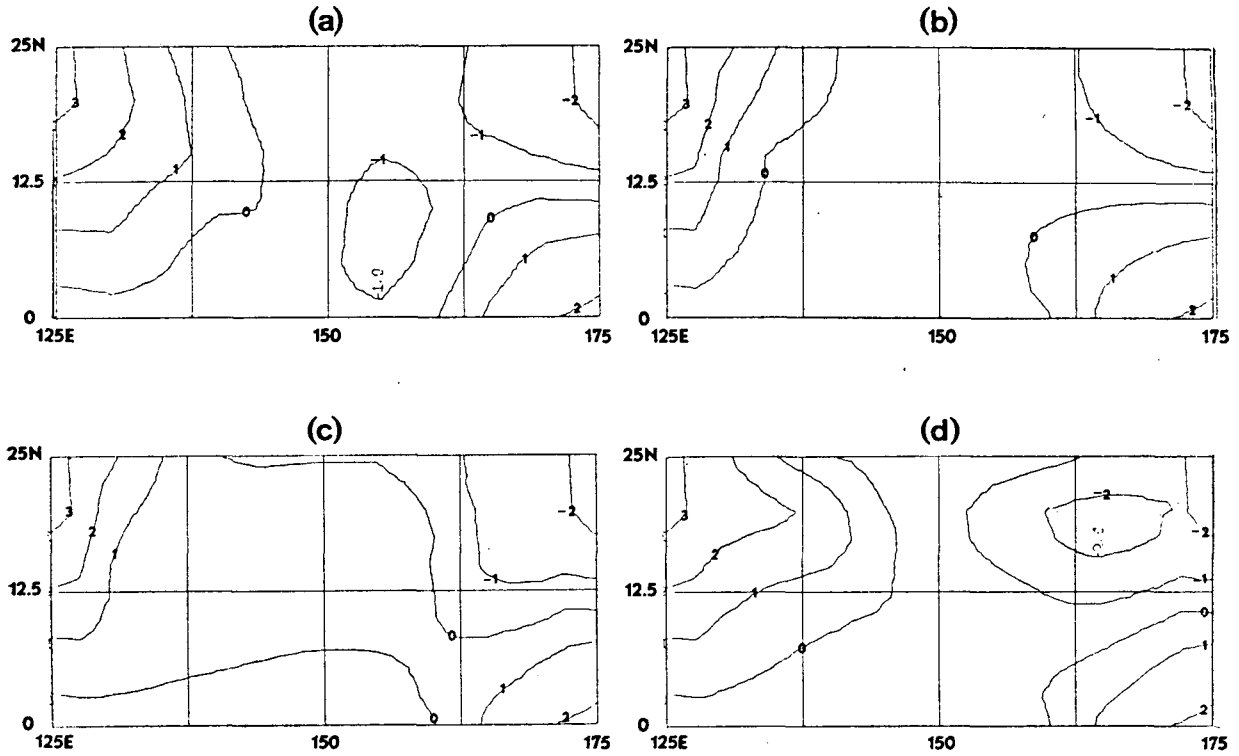

FIG. 7. Same as Fig. 3a–d, except for 6 August 71.

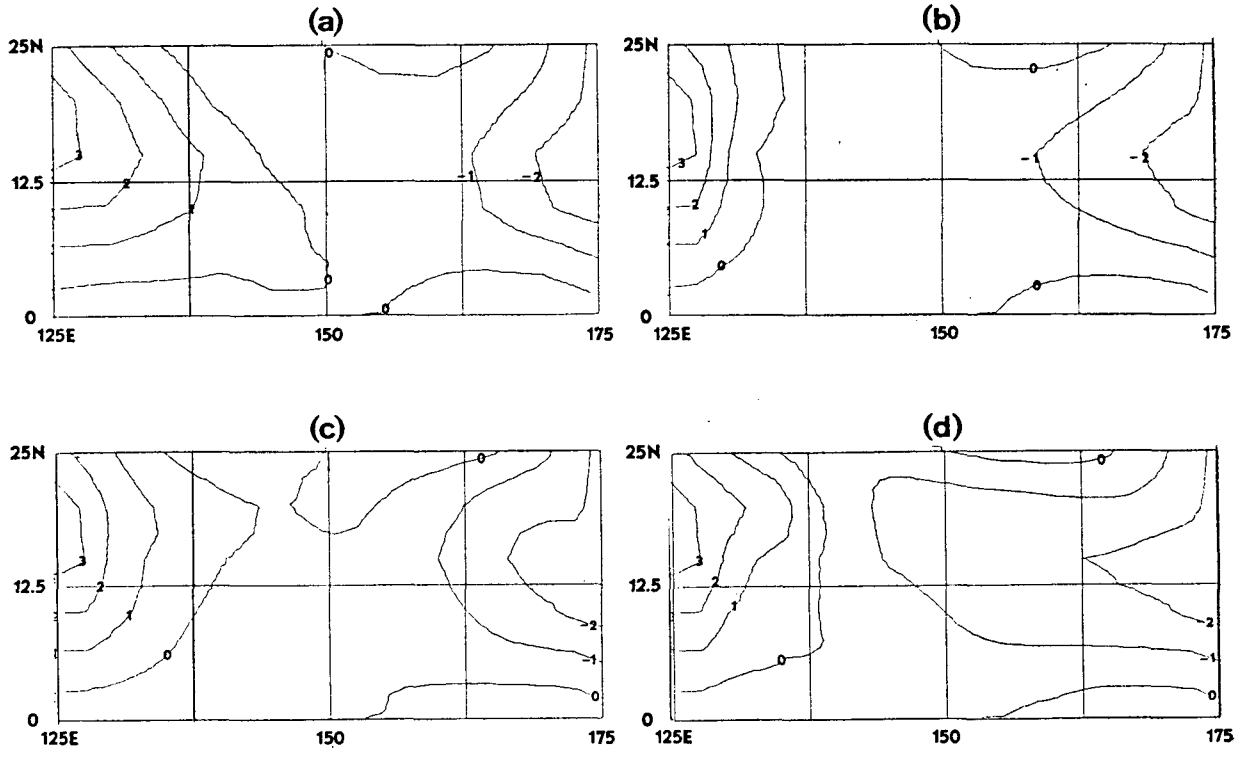

FIG. 8. Same as Fig. 3a–d, except for 7 August 71.

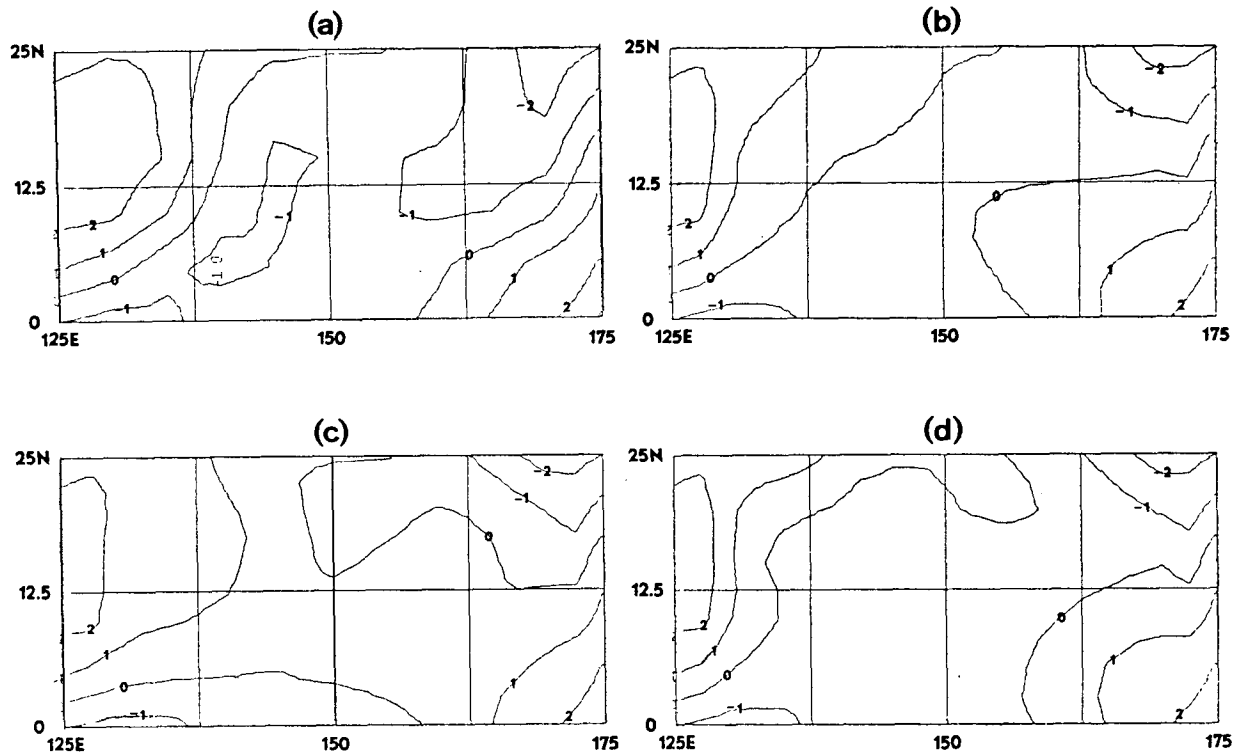

FIG. 9. Same as Fig. 3a–d, except for 9 August 71.

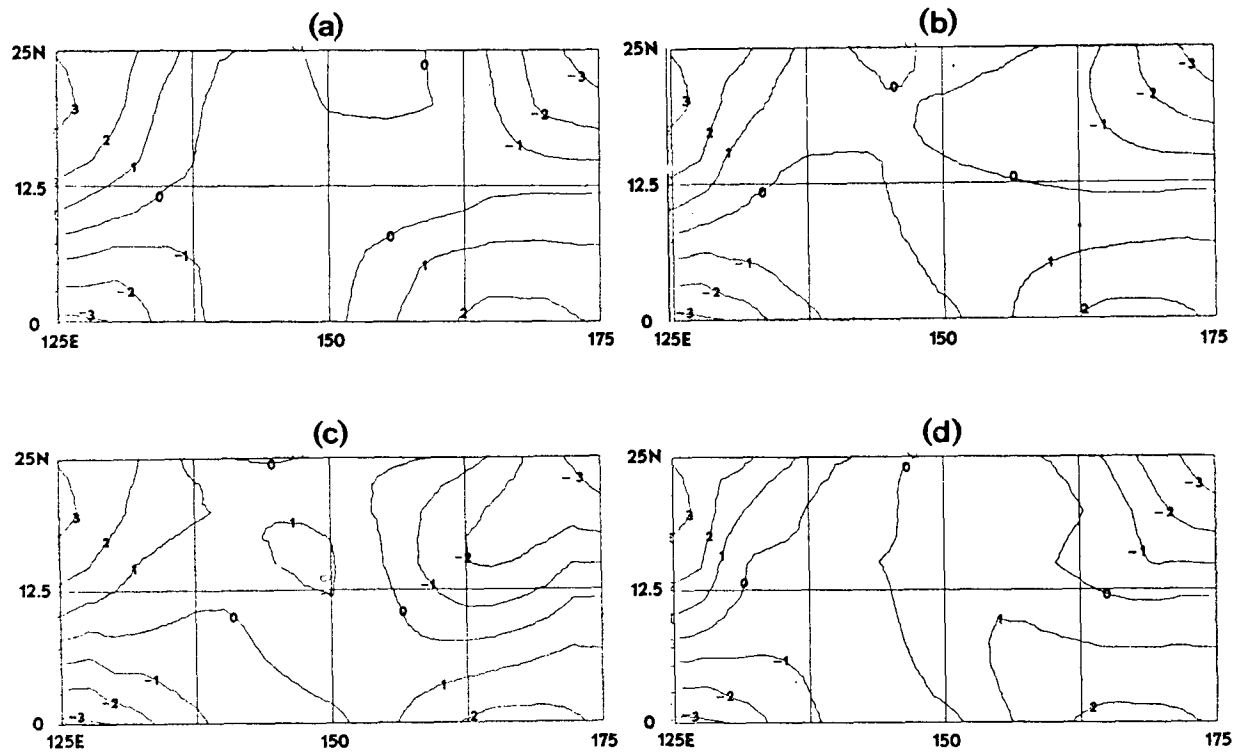

FIG. 10. Same as Fig. 3a–d, except for 10 August 71.

The results for 7 August are shown in Fig. 8. The correspondence between the brightness-forcing solution and the NMC field appears to be quite poor. However, closer examination reveals that the slope of the -1 contour produced by the brightness forcing closely approximates that of the zero contour of the NMC field, which is oriented NW-SE near the central western portion. Therefore, even though the appearance of the two fields differs considerably, the brightness-forcing solution still gives some useful information on the NW-SE flow direction in the central part of the test region, which is not the case for the fields obtained from divergence or zero forcing.

Both 9 and 10 August results as shown in Figs. 9–10 appear to depart greatly from the corresponding NMC fields. They are thus considered as two failing cases[2] of the model, although on 10 August the brightness forcing still seems to perform better than the divergence and zero forcings.

In summary, the above results show that the solutions obtained with the strong damping coefficient, $D=1.5\times10^{-5}$ s^{-1}, are generally more realistic than those obtained with $D=5\times10^{-6}$ s^{-1}. In the 8 days discussed, brightness forcing produced streamfunctions quite similar to the NMC field on two days (2 and 3 August) and gives useful information on the flow patterns on four days (4, 5, 6, and 10 August).

In addition to the solutions presented here, results were obtained for all days in the months of July and August for which data are available. Overall, for approximately 25% of the tested days, brightness forcing produces quite realistic streamfunctions resembling the NMC field, and in another 30% of the days it gives some useful information about the flow field. These results suggest that if no wind information is available over a tropical region, a first guess of the 200 mb flow field may be obtained from digitized satellite brightness data using a simple model such as that presented here.

Since the zero forcing results occasionally also give a rough sketch of the flow pattern, even steady-state solutions of the barotropic vorticity equation from boundary information alone may sometimes provide a guess of the flow that is better than nothing. This is especially true when divergence is weak as indicated by low brightness values. Thus it may be possible to use the steady-state, zero-forcing solution as another alternative to the current operational scheme for the data-void area.

b. Experiments with forcing modified by time-interpolated infrared data

Since the satellite digitized brightness does not supply direct information on the heights of the cloud clusters observed, the possible existence of low-level high brightness values may distort the upper-level flow pattern obtained from the solution of Eq. (2) under brightness forcing. If satellite infrared data (IR) were available for the same time and grid points as satellite cloud brightness data, the values of brightness could be modified according to the height of the cloud tops, which can be inferred from the IR data. This is because the condensation heating at upper levels is obviously related to the vertical extent of cumulus development. If accurate cloud-top temperatures and cloud-top heights can be determined, there may be ways to incorporate this information into the brightness data in order to distinguish the effects due to various vertical developments of cumulus convection. For example, since higher cloud tops are colder, we may assume that by giving higher weights to brightness values coincident with low IR readings the resultant field obtained by brightness forcing of Eq. (2) will better approximate the actual field. In this way the high brightness due to solar reflections at the surface would also be completely eliminated as far as the contribution to the divergence at the upper level is concerned.

In 1971, area-averaged, once-daily IR data from the NOAA-1 satellite over the 5°×5° latitude-longitude grids of the test region are available from NESS for the period 19 April–10 July. Unfortunately, the observation time is approximately 3 a.m. local time each day (or ~1200 GMT in the western Pacific), which is 12 hours different from that of the brightness data. However, although the life cycle of an individual cumulus element may be on the order of an hour or so, an organized cloud cluster with a scale on the order of the 5°×5° grid squares usually lasts several days or longer. Thus we decided to use the simple average of two consecutive IR observations to approximate the IR information at the brightness observation time. This interpolated data is then used to test the idea of enhancing the brightness forcing. Of course, this interpolation process may introduce large amounts of error, especially since cloud clusters are usually in a transient state with westward movement comparable to the speed of the zonal flow at low levels (Chang, 1970). Nevertheless, this crude representation of the IR data may provide us with some clue as to whether improvement can be reasonably expected in cases when actual IR data is available for use.

The NOAA-1 IR data period overlaps our experimental period only for the first ten days of July 1971; and, due to missing data in the IR tapes, only IR data for 4–5 July and 7–8 July can be used in our averaging procedure. Thus the "0000Z IR fields" are constructed for only two days: 5 July, which is the average of IR data of 4 July and 5 July; and 8 July, which is the average of 7 and 8 July. As done previously for the brightness and NMC data, these averaged IR data are further interpolated to give values at the 2.5°×2.5° grid points. A quite simple weighting scheme is then

[2] One of the reviewers pointed out that on these two days there were two tropical cyclones near the center of the area and that the NMC analysis is usually less reliable in such a situation.

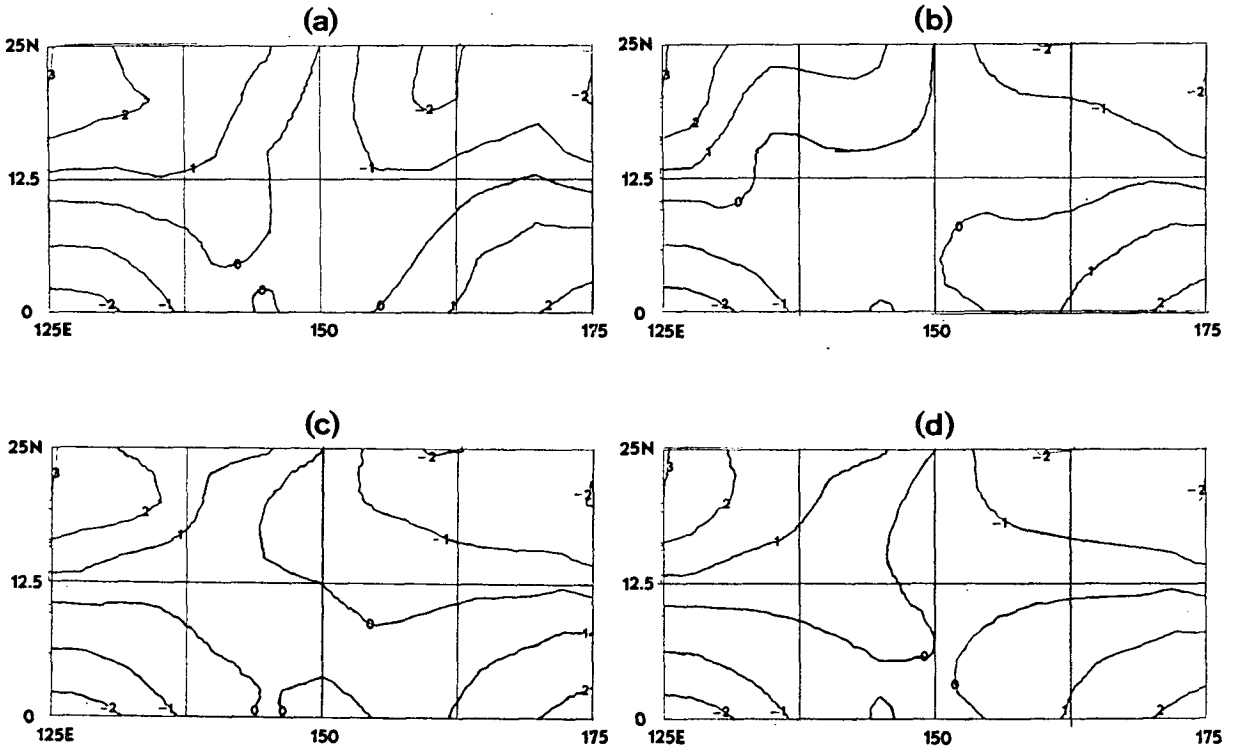

FIG. 11. Perturbation streamfunction at 200 mb for 5 July 71 (contour interval is 5×10^{6} s^{-1}). Fields shown are (a) the NMC-analyzed field; and the 72 h solutions with $D=1.5\times10^{-5}$ s^{-1} resulting from (b) divergence forcing, (c) brightness forcing, and (d) IR-modified brightness forcing.

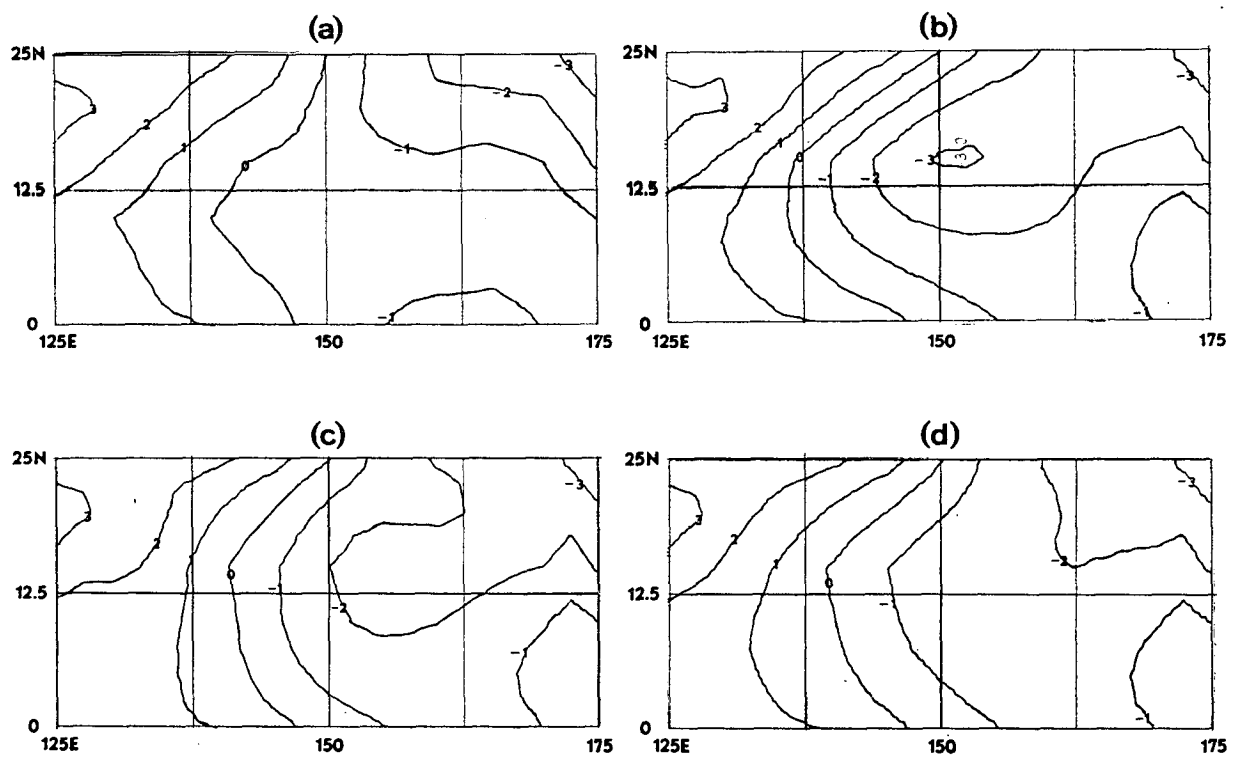

FIG. 12. Same as Fig. 11, except for 8 July 71.

used to modify the brightness values by the averaged IR field. This scheme, which is based on the facts that black-body radiation is proportional to the fourth power of the temperature while temperature varies almost linearly with height, is described by the following equation:

$$\left.\begin{aligned} CB_M &= (C - IR^{\frac{1}{4}})CB, \quad \text{if } C > IR^{\frac{1}{4}} \\ CB_M &= 0, \quad \text{if } C < IR^{\frac{1}{4}} \end{aligned}\right\}, \tag{4}$$

where

CB_M	IR-modified brightness
CB	original brightness
IR	averaged IR data
C	a parameter.

The parameter C is meant to represent the mean sea-surface temperature, which may have different values for different latitudes and is the fourth root of a high IR radiation reading at each latitude. For our simple testing, C is artificially determined at each latitude in the following manner:

1) The maximum IR value before averaging is determined for each day (4, 5, 7, and 8 July);

2) The minimum of these four maximum values is taken as the representative sea surface IR radiation; and

3) C is then set to equal the fourth root of the IR radiation.

The brightness data as modified by (4) are now transformed to the equivalent divergence field by the method described in Section 3. Equation (2), with $D = 1.5 \times 10^{-5}$ s^{-1}, is then used to obtain 72 h quasi-steady-state solutions for 5 and 8 July 1971, and compared with the results obtained previously. These are illustrated in Figs. 11 and 12, in which the following format is used:

a) the NMC-analyzed field,
b) the solution for divergence forcing,
c) the solution for brightness forcing, and
d) the solution for IR-modified brightness forcing.

Figure 11 shows the results for 5 July 1971. It can be readily seen that the gradients and pattern of the northwestern "high" area produced by the brightness forcing is improved by the IR modification and resembles the NMC field better. On 8 July 1971, which is shown in Fig. 12, significant improvement can again be found. In the center and center-east sections, the gradients produced by the IR modification are evidently closer to those of the NMC field than the unmodified forcing result. Thus our simple test suggests that there is great potential for the use of IR data to enhance the digitized brightness. The prospect in the future should be quite bright when concurrently-available IR data are used with brightness data, and when a better modification method is designed to replace (4).

5. Concluding remarks

The experiments carried out in this study suggest that, for data-sparse tropical regions, this model may be useful in obtaining a first estimate of the actual large-scale flow field from satellite data. This estimate may then be used to supplement whatever other information is available to improve the analysis in these regions.

The model proposed here may be improved in the future when better data and better understanding of the various physical processes of the large-scale tropical flow are available. For example, it is shown in two cases of this study that even with crude representations of the satellite IR data, the brightness forcing can be enhanced to produce more realistic flow patterns. Development in satellite technology should further improve the prospect of the model. Recently Allison *et al.* (1974) have shown that the Nimbus 5 Electrically Scanning Microwave Radiometer data may be combined with various IR and visible data to make several measurements that were not possible before. Among them are the differentiation between dense cirrus deck and rain areas and the detection of low-level water vapor concentration, which implies low-level convergence. Obviously, similar techniques can be used to define better the cumulus heating in the atmosphere. It may also be advantageous if the various types of area-averaged satellite data can become available at finer resolution, such as the $1° \times 1°$ latitude-longitude grids. Such data would also help the observational studies of tropical disturbances.

Better understanding of the physical processes may, on the other hand, enable us to improve the parameterization of the strong damping and the handling of the local time change term. It may also facilitate our knowledge of the relationships between satellite cloud data, condensation heating, and the resultant divergence and vertical motion. The scheme for specifying the forcing field from the various satellite data may then be greatly improved.

Acknowledgments. We wish to thank Messrs. S. Rinard and E. Varona for their assistance in data reduction, the reviewers for several valuable comments which result in significant improvement of the manuscript, and Prof. G. J. Haltiner for reading the final manuscript. Mr. Roy Jenne of the National Center for Atmospheric Research provided copies from NCAR tape library of the NOAA/NESS/MSL satellite brightness and the NOAA/NWS/NMC tropical wind data sets. Dr. Jay S. Winston of the Meteorological Satellite Laboratory provided the satellite infrared data. The basic idea for this research originated in a seminar discussion with Profs. J. M. Wallace and J. R. Holton at University of Washington, while one of us (CPC) was a student there. This research was supported by the National Environmental Satellite Service, National Oceanic and Atmospheric Administration, under Contract NA-833-73.

REFERENCES

Allison, L. J., E. B. Rogers, T. T. Wilheit, and R. W. Fett, 1974: Tropical cyclone rainfall as measured by the Nimbus 5 electrically scanning microwave radiometer. *Bull. Amer. Meteor. Soc.*, **55**, 1074–1089.

Ambroziak, R. A., 1973: An attempt to derive the 200 mb wind field from digitized cloud brightness data. M.S. Thesis, University of Washington, Seattle, 30 pp.

Chang, C.-P., 1970: Westward propagating cloud patterns in the tropical Pacific as seen from time-composite satellite photographs. *J. Atmos. Sci.*, **27**, 133–138.

Hawkins, H. F., and S. L. Rosenthal, 1965: On the computation of streamfunctions from the wind field. *Mon. Wea. Rev.*, **93**, 245–252.

Hayashi, Y., 1974: Spectral analysis of tropical disturbances appearing in a GFDL general circulation model. *J. Atmos. Sci.*, **31**, 180–218.

Holton, J. R., 1972: *An Introduction to Dynamic Meteorology*. New York, Academic Press, 319 pp.

——, and D. E. Colton, 1972: A diagnostic study of the vorticity balance at 200 mb in the tropics during the northern summer. *J. Atmos. Sci.*, **29**, 1124–1128.

Martin, D. W., and W. D. Scherer, 1973: Review of satellite rainfall estimation methods. *Bull. Amer. Meteor. Soc.*, **54**, 661–674.

Nitta, T., 1972: Structure of wave disturbances over the Marshall Islands during the years of 1956 and 1958. *J. Meteor. Soc. Japan*, **50**, 85–103.

Reed, R. J., and R. H. Johnson, 1974: Diagnosis of cloud population properties in tropical easterly waves. Preprints, International Tropical Meteorology Meeting, Nairobi, 50–55.

——, and E. E. Recker, 1971: Structure and properties of synoptic scale wave disturbances in the equatorial western Pacific. *J. Atmos. Sci.*, **28**, 1117–1133.

Sangster, W. E., 1960: A method of representing the horizontal pressure force without reduction of station pressure to sea level. *J. Meteor.*, **17**, 166–176.

Shukla, J., and K. R. Saha, 1974: Computation of non-divergent streamfunction and irrotational velocity potential from the observed winds. *Mon. Wea. Rev.*, **102**, 419–425.

Varona, E., 1974: A comparative study of digitized brightness and 200-mb divergence in the tropical western North Pacific. M. S. Thesis, Naval Postgraduate School, Monterey, Calif., 49 pp.

Wallace, J. M., 1970: Time-longitude sections of tropical cloudiness (Dec. 1966–Nov. 1967). ESSA Tech. Report, NESC 56, Washington, D. C., 37 pp.

——, 1971: Spectral studies of tropospheric wave disturbances in the tropical western Pacific. *Rev. Geophys. Space Phys.*, **9**, 557–612.

Williams, K. T., and W. M. Gray, 1973: Statistical analysis of satellite-observed tradewind cloud clusters in the western North Pacific. *Tellus*, **25**, 313–336.

Yanai, M., S. Esbensen, and J.-H. Chu, 1973: Determination of bulk properties of tropical cloud clusters from large-scale heat and moisture budgets. *J. Atmos. Sci.*, **30**, 611–627.